arXiv:1403.5356v2 [physics.flu-dyn] 24 Mar 2014

Complexity and Prediction in 2D Turbulence

R.T. Cerbus[1,2,*] and W.I. Goldburg[1]

[1]*Department of Physics and Astronomy, University of Pittsburgh, 3941 O'Hara Street, Pittsburgh PA 15260*
[2]*Fluid Mechanics Unit, Okinawa Institute of Science and Technology Graduate University, Okinawa 904-0495, Japan*

Information theory is employed to quantify the complexity of experimental data from a turbulent soap film. The statistical complexity C is a measure of the cost of prediction, *i.e.* the amount of information necessary to make it. The excess entropy E is the system's memory. The formalism reveals a transition when the system changes its behavior as a turbulent cascade develops. After this, C decreases while E increases as the Reynolds number Re increases. They eventually become equal at an asymptotic state. The behavior of C and E as a function of Re provides new insights into the behavior of turbulence.

Turbulence is the fruit fly of complex systems, but its degree of complexity has not been a subject of study. In this Letter, we will address the issue of complexity in experimental data from a turbulent soap film. The starting point is Shannon's information theory [1–3], where, in Neil Gershenfeld's words, "...information is what you don't already know" [4]. With this in mind, every experiment conveys a stream of information about the physical state of the system. The statistical complexity C proposed by Crutchfield and coworkers [5, 6] is the minimum amount of information needed to model the system, *i.e.* reproduce the system's behavior statistically (same probability distributions). It is determined without invoking any model and with a minimum of assumptions [7]. It is also intimately connected with the idea of a physical system processing information [5, 8–11].

In a previous work we have used Shannon's entropy density h, the amount of new information revealed by each measurement, to characterize the randomness or instrinsic uncertainty of 2D turbulence in a flowing soap film as a function of Reynolds number Re [12]. In this Letter we use C to characterize the same system. Doing so has suggested several insights for 2D turbulence. (1) The presence of a cascade leaves its signature on C, since it reduces the amount of information needed to predict the system's behavior. (2) 2D turbulence becomes increasingly easy to predict (less complex) as Re increases. (3) The quantities C and E, the system's memory, appear to approach a common constant value at finite Re.

We now provide a more detailed description of these ideas. A mathematically involved treatment can be found in Ref. [7] while an overview can be found in Ref. [5]. In the discussion that follows, an uppercase letter denotes a set of variables and a lowercase letter denotes a particular member of the set. Consider a stationary experimental spatial series $U_x = (...U_{x-1}, U_x, U_{x+1}, ...)$, where U is the vertical component of the velocity in the soap film. The members of U_x belong to a set of discrete variables with some probability distribution $P(U)$. Information from the past $\overleftarrow{U} = (...U_{x-3}, U_{x-2}, U_{x-1})$ is transferred to the future $\overrightarrow{U} = (U_x, U_{x+1}, U_{x+2}...)$ through the present. For a 1D spatial series of data such as the one considered here, the past and future become "left" and "right", although the formalism is identical. An excellent example of these ideas applied to a spatially extended system is the spin systems in Ref. [13].

We need to determine a set of special states called causal states S [5]. These will make up a minimal representation of our system for predictive purposes. In a different parlance, we are trying to build a (possibly hidden) Markov model [14]. To determine S, consider all unique blocks of data U^L *i.e.*, a sub-string of adjacent in space data values of length L. One would like to make L large to capture as many correlations as possible, but the finite amount of data means only finite L can be statistically reliable. In practice, only a finite L is necessary anyway. With a large amount of data, we can calculate the conditional probability that any one past block $\overleftarrow{u}^L$ will give rise to any other future block of the same length: $P(\overrightarrow{U}^L|\overleftarrow{u}^L)$. If the conditional probability distributions of any future blocks $\overrightarrow{U}^L$ are the same, they are said to cause the same future. From a statistically predictive point of view they are equivalent. Thus block 1 and block 2 are equivalent, $u_1^L \sim u_2^L$, if $P(\overrightarrow{U}^L|\overleftarrow{u}_1^L) = P(\overrightarrow{U}^L|\overleftarrow{u}_2^L)$.

All equivalent blocks are then combined into a single causal state. We now have a set of predictive causal states S. The Shannon information (entropy) contained in S is the statistical complexity

$$C = H[S] = -\sum_s P(s)\log_2 P(s), \tag{1}$$

where the logarithm is taken to the base 2, giving units of "bits". For our turbulent velocity field, this is the total amount of information needed to statistically reproduce the data.

When actually handling real data to identify S, we must deal with imperfections. These imperfections may be due to external noise or the finiteness of the amount of data, *etc.* Regardless of the origin, some threshold needs to be set to determine if two conditional probability distributions for the future are the same, since they will never be identical. An example of some conditional probability distributions is shown in Fig. 1. Two of the distributions are similar, indicating that the two states

belong to the same causal state. The third distribution is entirely different. The task is to choose a sensible metric to make this distinction objectively.

This problem was apparently also recognized by the creators of this complexity machinery, although reference to it is apparently absent in previous literature [5, 6, 13–16]. They developed the Causal State Splitting Reconstruction (CSSR: pronounced "scissor") algorithm, which is outlined in Ref. [17] and is available for download from its author's website [18].

We developed a MATLAB program that uses either a χ^2 or a Kolmogorov-Smirnov test to compare any two conditional probability distributions and determine S [19]. A 0.95 confidence level is used, but the results are not sensitive to this parameter. The CSSR algorithm and our own method are in good agreement. In the end, of course, choosing a suitable metric for determining the causal states has an element of subjectivity to it.

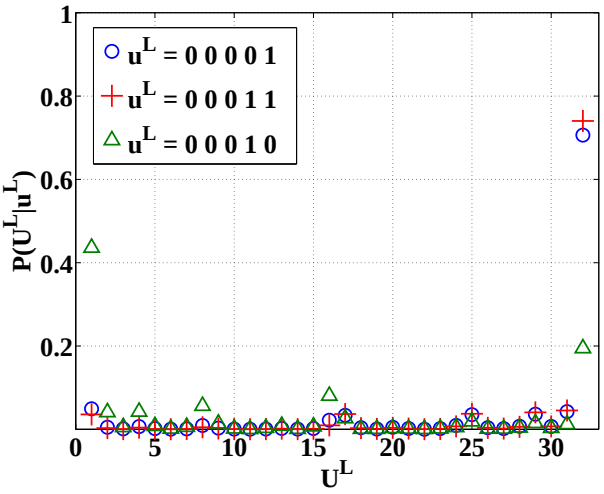

FIG. 1: An example of three conditional pdfs used to determine the causal states. The data used here is binarized turbulence data with $L = 5$ (giving a total of 32 possible states) and $Re = 3300$ ($\bigcirc = 00001$, $+ = 00011$, $\triangle = 00010$). The horizontal axis features all the possible future states while the vertical axis is the conditional probability that given a certain past state, any of those possible future states will occur. Here the distribution for states $\bigcirc$ and $+$ appear similar while that for state $\triangle$ is quite different. For example, on the far right $P(U^L|\bigcirc)$ and $P(U^L|+)$ are basically the same while $P(U^L|\triangle)$ is quite different. The χ^2 test confirms what the eye sees: $\bigcirc$ and $+$ belong to the same causal state while $\triangle$ does not.

While C is the total amount of information needed to predict the future, the amount of information that is actually communicated between the past and future is the excess entropy E [15, 16]. It is simply defined as the mutual information shared between the past and future [15, 16]:

$$E = I[\overleftarrow{U}; \overrightarrow{U}] = I[S; \overrightarrow{U}] = \lim_{L\to\infty} \sum_{L} (h_L - h), \qquad (2)$$

where $h_L = H(U^{L+1}) - H(U^L)$ [20, 21]. For our spatial velocity data we interpret E as a memory. This quantity measures how much the "left" knows about the "right", so it is also a measure of the strength of correlations.

Estimating E involves the Shannon entropy rate (density) h, which is defined as [5, 15]

$$h = H[\overrightarrow{U}^1|\overleftarrow{U}] = H[\overrightarrow{U}^1|S] = \lim_{L\to\infty} h_L, \qquad (3)$$

where the second equal sign gives the relation to the causal states S. This definition of h points to the sufficiency of S to describe the system.

To estimate h and E, we use standard techniques involving the block entropies $H(U^L)$ used in the third equal sign of Eq. 2 and the third equal sign of Eq. 3 [12, 20, 21]. The undersampling bias in the $H(U^L)$ is corrected using Grassberger's method [20], although this did not affect the values of h and E very much. We also used the fact that for many chaotic systems, $h_L - h \propto 2^{-\gamma L}$ (γ is some constant independent of L) to better estimate E when possible [21]. The results for h were compared with the results from the second equal sign of Eq. 3 as a check. More details on the inter-relationships between h, E, C and other quantities can be found in Ref. [15, 16].

As a simple illustration of these ideas, consider a coin flipping experiment where each subsequent flip will be the same as the previous one with probability $p \in [0, 1]$ [10]. If $p = 0.5$, we have the usual fair coin toss experiment, with $h = 1$ and $C = E = 0$, since this system is maximally uncertain but statistically simple to predict with no information being shared between the past and future. If p deviates from 0.5 even slightly, $C = 1$ since we will always need to know 1 bit of information (the previous coin flip) to predict the future. For a small deviation from 0.5 such as $p = 0.55$, $h \simeq 0.95$ and $E \simeq 0.05$. Thus, if our system is "nearly" random with only weak correlations, h and E hardly deviate at all from their random values ($h = 1$, $E = 0$). This example also highlights the difference between E and C, the crypticity $\chi = C - E$ ($= h$ in this example) [14, 15]. This is the amount of information necessary to predict the system's future behavior above that which is actually transmitted or observed (E). This is in stark contrast to periodic systems where $E = C = \log_2 T$, where T is the (dimensionless) period [5]. In these systems, the period is both all that is needed to predict the future of the system and at the same time is the information shared between the past and the future.

In order to use this formalism with turbulence, the continuous experimental data must be converted to symbols [22]. A partition is defined which assigns data values in

a specified range to a unique symbol [20, 22]. (In some sense all experiments do this because of their limited precision.) There are numerous previous studies where even binarizing a turbulent velocity signal has given more insight than traditional techniques [12, 22–24]. In a previous study of h for this same system, we showed that binarizing led to results very similar to that for much finer partitions [12]. (Binarizing the data here means translating a data value to 0 if it is below the mean velocity and 1 otherwise.)

In this work we primarily use a binary partition, since this smaller alphabet allows us to use a larger L, which enables us to cover a wider range of length scales in our analysis. We think of this binarization as a diagnostic tool. The behavior of a sequence of these 0s and 1s determined by the turbulent velocity tells us about the turbulence itself. Just as with h in Ref. [12] we have found that the general behavior with respect to Re is independent of the partition size.

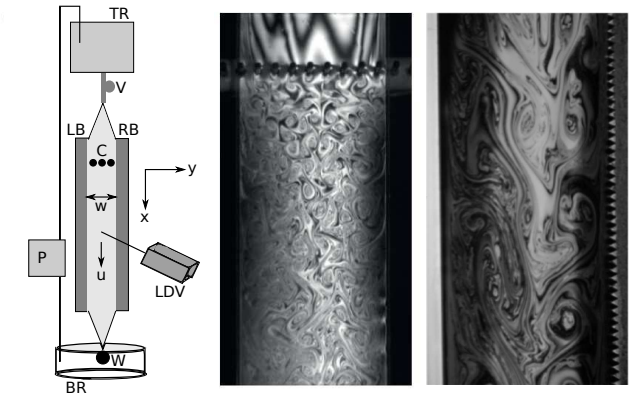

FIG. 2: Left: Experimental setup showing the reservoirs (TR, BR), pump (P), valve (V), comb (C), blades (LB, RB), LDV and weight (W). Middle: Fluctuations in film thickness from turbulent velocity fluctuations with smooth walls and a comb. Right: Thickness fluctuations with smooth and rough wall. (Figure adapted from [25].)

Now consider a turbulent soap film, which is a good approximation to 2D turbulence since the film is only several μm thick [26, 27]. The soap solution is a mixture of Dawn (2%) detergent soap and water with 4 μm particles added for laser doppler velocimetry (LDV) measurements. Figure 2 is a diagram of the experimental setup.

The soap film is suspended between two vertical blades connected to a nozzle above and a weight below by nylon fishing wire. The nozzle is connected by tubes to a valve and a reservoir which is constantly replenished by a pump that brings the spent soap solution back up to the reservoir. The flow is gravity-driven. Typical centerline speeds $\overline{u}$ are several hundred cm/s with rms fluctuations u' ranging from roughly 1 to 30 cm/s. The channel width w is usually several cm. The Reynolds number $Re = u'w/\nu$, where ν is the kinematic viscosity, thus ranges from 10 to 10,000.

Turbulence in the soap film is generated by either (1) inserting a row of rods (comb) perpendicular to the film or (2) replacing one or both smooth walls with rough walls (saw blades), with the comb removed. When protocol (1) is used we almost always observe the direct enstrophy cascade [26, 27]. If procedure (2) is used, we can observe an inverse energy cascade [26–28]. The ability to see the inverse energy cascade depends sensitively on the flux and channel width. The type of cascade is determined by calculating the one-dimensional velocity energy spectrum $\mathcal{E}(k)$, where $\frac{1}{2}u'^2 = \int_0^\infty \mathcal{E}(k)dk$. For the enstrophy cascade, $\mathcal{E}(k) \propto k^{-3}$ and for the energy cascade $\mathcal{E}(k) \propto k^{-5/3}$. A number of measurements were taken near the top of the channel where the flow is still quite slow. In this case $\mathcal{E}(k)$ is flat and there is no power-law scaling and so apparently no cascade, although the flow is not truly laminar ($u' \neq 0$).

In all cases, we measure the longitudinal (streamwise) velocity component at the horizontal center of the channel. The data rate is $\simeq$ 5000 Hz and the time series typically had more than 10^6 data points. With this high data rate, the smallest turbulent scales seem to be resolved. For this system, the time series is really a spatial series by virtue of Taylor's frozen turbulence hypothesis [26, 27, 29]. This is an important distinction, as discussed in Ref. [12].

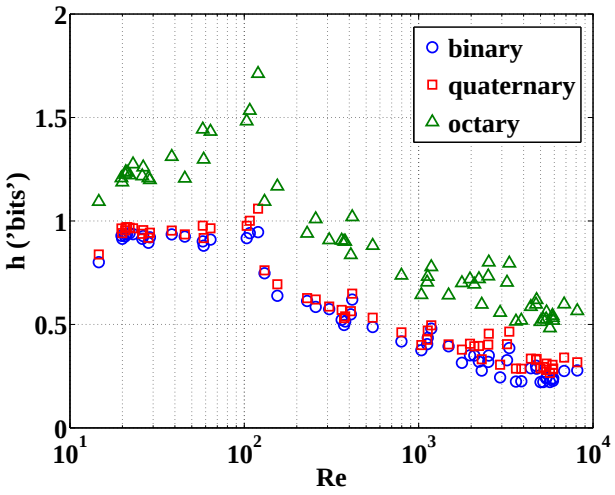

FIG. 3: The entropy density h plotted vs. Re for three different alphabet sizes. Binary (◯), quaternary (□) and octary (△) alphabets were used. Except for a vertical shift, all three treatments show the same behavior with respect to Re.

We now recall a recent result where the entropy density h is estimated for 2D turbulence data [12]. Using two different methods, h is shown to be a logarithmically decreasing function of Re. We reproduce these results

here in Fig. 3 to also illustrate that this h vs. Re behavior is independent of the partition (alphabet) size. The decrease in h is presumably connected with the increased correlations [2] inherent in a turbulent cascade. However, h is not a direct measure of correlations but of randomness or uncertainty [30].

In order to dig deeper into turbulent cascades, at least for 2D turbulence, we must use the ideas outlined previously. The quantities C and E are plotted vs. Re in Fig. 4. C was calculated using our MATLAB program and the χ^2 test. We used $L = 10$ which is similar to the L used to calculate h and E for each case [12]. The data are cleanly divided in Re into no-cascade, energy and enstrophy regimes.

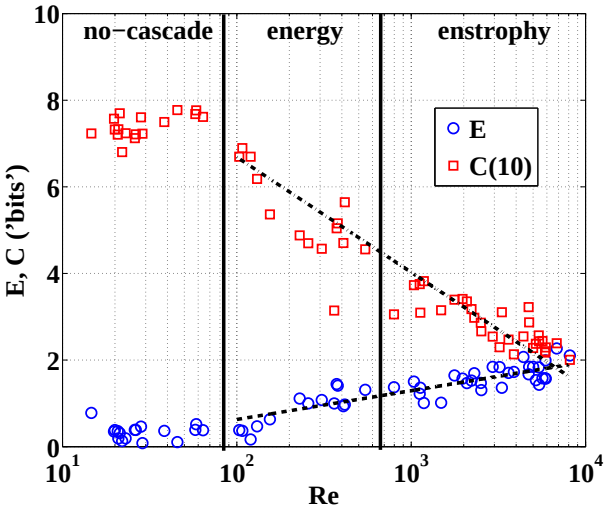

FIG. 4: The statistical complexity C and excess entropy E as a function of Re. Here $L = 10$ and our MATLAB program using the χ^2 test was used to calculate C. The lines are not fits to the data but are meant to suggest the behavior of C and E as functions of Re. One can see that after the initial "hump", C is a decreasing function of Re while E increases. E and C appear to reach a common value, which suggests an asymptotic state of 2D turbulence at finite Re. The vertical lines roughly separate the data according to their cascade. Here the separation of the energy and enstrophy cascades in Re should be thought of as a feature of the experiment and not something more fundamental.

Focusing on Fig. 4, we first notice that C changes its behavior with Re. It is initially roughly constant and then decreases logarithmically with Re when a cascade develops. This change in behavior is different from the laminar to turbulent transition usually discussed (*e.g.* pipe flow), where one focuses on the onset of fluctuations, which do not constitute turbulence in its mature, fully-developed sense [29]. (For laminar flow, $h = E = C = 0$, since the experimental data would be a single unchanging value.) The fluctuations of pre-cascade turbulence are apparently difficult to predict (C is large in Fig. 4). However, if the fluctuations belong to a cascade, the information needed to predict the system's behavior is less.

Significantly, E is an increasing function of Re. In other words, the turbulence has an increasing amount of spatial memory as it grows in strength. This is fully compatible with the usual notion that as Re increases, more correlated degrees of freedom participate in the cascade. On the other hand, C is simultaneously decreasing with Re, which indicates that the turbulent system is becoming easier (statistically) to model. Contrary to intuition, high Re turbulence is less complex than low Re turbulence. Moreover, one might be tempted to interpret the reduction in C as the system's approach to simple white noise. However, since h decreases and E increases at the same time, this can not be the case (for white noise, $h = 1$ and $C = E = 0$).

A simple, qualitative interpretation of this result is that as more and more eddy sizes are joining the cascade, the large inertial range dominates the behavior of the system. This statistical structure which leads to power laws in $\mathcal{E}(k)$ also shows up as a reduction in C. The crypticity, $\chi = C - E$, is clearly nonzero and decreases with Re. The experiments show that as $Re \to \infty$, only E is needed to predict the future. No more hidden information (χ) is needed. If we turn to a complementary interpretation of C and E, we are seeing that our system is becoming logically and computationally reversible [31].

Since $\chi \geq 0$ [14, 15], C and E will apparently not change in value after meeting. (Incidentally, their meeting is independent of L and partitioning.) This limiting value for E and C suggests that there is a kind of limiting state that can be reached at a finite value of Re. This is a notable inference that can be drawn from this experiment.

We would like to thank D. P. Feldman for explaining several of these concepts to us and for making his excellent lecture notes available online. We are also grateful to K. L. Shalizi and C. R. Shalizi for making the CSSR algorithm implementation freely available online. C. J. Ellison was kind enough to explain some of the finer points of this formalism to us. We are also indebted to M. Bandi for providing numerous suggestions and insights. This work is supported by NSF Grant No. 1044105 and by the Okinawa Institute of Science and Technology (OIST). R.T.C. is also supported by a Mellon Fellowship through the University of Pittsburgh.

* Electronic address: rtc17@pitt.edu

[1] C. E. Shannon, W. Weaver, *The Mathematical Theory of Communication* (University of Illinois Press, Urbana, 1964)

[2] T. M. Cover, J. A. Thomas, *Elements of Information Theory* (Wiley, New York, 1938)

[3] L. Brillouin, *Science and Information Theory* (Academic Press, New York, 1962)
[4] N. Gershenfeld, *The Physics of Information Technology* (Cambridge University Press, Cambridge, 2000)
[5] J. P. Crutchfield, Nat. Phys. **8**, 17 (2012)
[6] J. P. Crutchfield, K. Young, Phys. Rev. Lett. **63**, 105 (1989)
[7] C. R. Shalizi, J. P. Crutchfield, J. Stat. Phys. **104**, 817 (2001)
[8] S. Lloyd, Nature **406**, 1047 (2000)
[9] R. Landauer, Phys. Lett. A **217**, 188 (1996)
[10] R. Quax, A. Appolloni, P. M. A. Sloot, Eur. Phys. J. Spec. Top. **222**, 1389 (2013)
[11] R. S. Shaw, Z. Naturforsch **36A**, 80 (1981)
[12] R. T. Cerbus, W. I. Goldburg, Phys. Rev. E **88**, 053012 (2013)
[13] J. P. Crutchfield, D. P. Feldman, Phys. Rev. E **55**, R1239 (1997)
[14] J. R. Mahoney, C. J. Ellison, R. G. James, J. P. Crutchfield, Chaos **21**, 037112 (2011)
[15] C. J. Ellison, J. R. Mahoney, J. P. Crutchfield, J. Stat. Phys. **136**, 1005 (2009)
[16] J. P. Crutchfield, C. J. Ellison, J. R. Mahoney, Phys. Rev. Lett. **103**, 094101 (2009)
[17] C. R. Shalizi, K. L. Shalizi, J. P. Crutchfield, arXiv:cs/0210025v3 [cs.LG]
[18] *http* : *//vserver*1.*cscs.lsa.umich.edu/ crshalizi/CSSR/*
[19] E. L. Lehmann, J. P. Romano, *Testing Statistical Hypotheses, 3rd Ed.* (Springer, New York, 2005)
[20] T. Schürmann, P. Grassberger, Chaos **6**, 414 (1996)
[21] J. P. Crutchfield, D. P. Feldman, Chaos **13**, 25 (2003)
[22] C. S. Daw, C. E. A. Finney, E. R. Tracy, Rev. Sci. Instrum. **74**, 915 (2002)
[23] A. J. Palmer, C. W. Fairall, W. A. Brewer, IEEE Trans. Geo. Remote Sensing **38**, 2056 (2000)
[24] M. Lehrman, A. Rechester, Phys. Rev. Lett. **87**, 164501 (2001)
[25] T. Tran, P. Chakraborty, N. Guttenberg, A. Prescott, H. Kellay, W. I. Goldburg, N. Goldenfeld, G. Gioia, Nat. Phys. **6**, 438 (2010)
[26] H. Kellay, W. I. Goldburg, Rep. Prog. Phys. **65**, 845-894 (2002)
[27] G. Boffetta, R. Ecke, Ann. Rev. Fluid Mech. **44**, 427 (2012)
[28] H. Kellay *etal.*, Phys. Rev. Lett. **109**, 254502 (2012)
[29] P. A. Davidson, *Turbulence: An Introduction for Scientists and Engineers* (Oxford University Press, Oxford, 2004)
[30] D. P. Feldman, J. P. Crutchfield, Phys. Lett. A **238**, 244 (1998)
[31] K. Wiesner, M. Gu, E. Rieper, V. Vedral, Proc. Roy. Soc. A **468**, 4058 (2012)